Journal of Electron Devices, Vol. 20, 2014, pp. 1777-1785

© JED [ISSN: 1682 -3427]

Journal of Electron Devices
www.jeldev.org

STUDY OF DRAIN CURRENT FOR AlGaN/GaN SUPERLATTICE MOSFET CONSIDERING VARIOUS SCATTERING IN NON-EQUILIBRIUM STATE

Kaushik Mazumdar[1], Saddam Hussain[1], Jitendra Kumar[1], Aniruddha Ghosal[2]
[1]Indian School of Mines (I.S.M.), Dhanbad–826004, Jharkhand.
[2]Institute of Radio Physics and Electronics, University of Calcutta, 92, A.P.C. Road, Kol–700009.
kaushik_edu@yahoo.co.in

Received 30-10-2014, online 3-11-2014

ABSTRACT

The variation of mobility with lattice temperature due to lattice vibrations, impurities, and interface roughness in GaN quantum well has been studied. The variation of conductivity and power dissipation with lattice temperature in AlGaN/GaN superlattice has been studied taking into account both bulk and superlattice phonon interactions with electrons. The conductivity and power dissipation in AlGaN/GaN superlattice is highest at 45K for both bulk and superlattice phonons. Also the drain current in terms of lattice temperature in AlGaN/GaN superlattice MOSFET has been studied for both superlattice and bulk phonons.

I. INTRODUCTION

The study of transport phenomena in large band gap semiconductor (GaN)-based quantum wells (QWs) in MOSFETs and its effects is stimulating and interesting field of research for many years [1-7]. There is no doubt that using the improving technique, a good quality GaN/AlGaN QW be produced in which the scattering of the electrons by temperature is dominant mechanism. In previous investigations [1-3] of electron transport mechanism and its various aspects were performed in AlGaAs/GaAs superlattice MOSFET near equilibrium electron state i.e. in very low electric field. In this paper, authors have studied transport phenomena and its effects on mobility, conductivity, power dissipation and drain current based on lattice temperature in GaN-based quantum wells of MOSFETs under non-equilibrium conditions i.e. at very high electric field and have compared that of the various effects of transportation mechanism in bulk material. Here the deformation acoustic (DA) and piezoacoustic (PA) phonons interaction with polar optical (PO) phonons, background impurities (BI) and remote impurities (RI), and with the quantum well interface roughness (IR) are taken into account for various aspects. It is assumed that the electron gas is non-degenerate and the electron average kinetic energy ϵ and the lattice temperature T satisfied the conditions $(K_0T, \epsilon) < \hbar\omega_0$, where $\hbar\omega_0$ is the optical phonon energy. These conditions impose an upper limit on both the external electric field **E** and the lattice temperature T. Since for GaN the optical phonon energy is large, $\hbar\omega_0 \approx 1100$ K, this condition can be satisfied within a wide range of actual E and T. Ongoing beyond the electron temperature approximation, here a set of distribution functions [4] is used for non-equilibrium electrons in GaN-based QWs with many electron subbands included to find momentum relaxation time of electrons due to different scattering.

II. MOMENTUM RELAXATION TIMES OF 2D ELECTRONS

Here consider a two-dimensional (2D) electron gas confined in infinitely deep square GaN quantum well (QW) of thickness L subject to an external electric field **E** parallel to quantum layers. The energy dispersion of the QW electrons with in-plane wavevector $\boldsymbol{k}_{\|}$ in subband *n* is $\epsilon_n(\boldsymbol{k}_{\|}) = \frac{\hbar^2 k_{\|}^2}{2m^*} + W_0 n^2$ with n = 1, 2 . . . , where $W_0 = \pi^2\hbar^2/2m^*L^2$, $\hbar = h/2\pi$, *h* is Plank's constant and *m** is the electron effective mass. In order to calculate the kinetic coefficients of the non-equilibrium electron gas it is necessary to know the electron distributions function $F_n(\boldsymbol{k}_{\|})$ which is governed by the Boltzmann kinetic equation

$$-\frac{e\mathbf{E}}{\hbar}\frac{dF_n(\boldsymbol{k}_{\|})}{d\boldsymbol{k}_{\|}} = \sum_{i=1}^{3} \hat{\mathrm{I}}^{(i)} F_n(\boldsymbol{k}_{\|}) \qquad (1)$$

where $\hat{\mathrm{I}}F_n(\boldsymbol{k}_{\|})$ is a scattering operator which describes the interaction between electrons and the scatterers with wave vector $\mathbf{q} = (\mathbf{q}_{\|}, \mathbf{k}_{\perp})$ and frequency $\omega_\lambda(\mathbf{q})$. The scattering probability $\mathrm{w}_i(\boldsymbol{q})$ due to interaction with DA (i=1), PA (i=2) and PO (i=3) are given respectively: $\mathrm{w}_1(\boldsymbol{q}) = \left(\frac{\pi E_a^2}{\rho V_0 s_L}\right) q$, $\mathrm{w}_2(\boldsymbol{q}) = \left(\frac{\pi e^2 h_{14}^2}{\rho V_0 s_T}\right) C_\lambda(\boldsymbol{e}_q) q^{-1}$, $\mathrm{w}_3(\boldsymbol{q}) = \left(\frac{4\pi e^2\omega_0}{V_0}\right)(\epsilon_\infty^{-1} - \epsilon_0^{-1})$, where E_a is the deformation potential constant, h_{14} is the piezoelectric constant, $\epsilon_0, \epsilon_\infty$ are the low and high frequency dielectric constants, ρ is the material density, V_0 is the volume of the QW and $\boldsymbol{e}_q = \frac{\boldsymbol{q}}{q}$, s_λ is the longitudinal (λ = L) or transverse (λ = T) acoustic velocity. The scattering probability $\mathrm{w}_2(\boldsymbol{q})$ by PA phonons depends in general on the orientation of $\boldsymbol{q}$ with respect to the crystal axes [5] through the factor $C_\lambda(\boldsymbol{e}_q)$ and on the crystal structure of GaN (zinc-blende or wurtzite). As a result $\mathrm{w}_2(\boldsymbol{q})$ for 2D electrons in a QW depends on the orientation of the interfaces of the QW with respect to the crystal axes. Here we used the PA-isotropy model in which it is assumed that for a cubic crystal $C_L(\boldsymbol{q})$ = 0 and $C_T(\boldsymbol{q})$ = 1. Thus our results are more relevant to zinc-blende than the wurtzite structure of GaN. For interaction with background impurities (BI) (i=4), remote impurities (RI) (i=5), and QW interface roughness (IR) (i=6), all of which are elastic, the scattering probability is given by $\mathrm{w}_{4,5}(\boldsymbol{q}_{\|}) = \left(\frac{4\pi^2 n_s e^4}{A_0\epsilon_0^2}\right)\boldsymbol{q}_{\|}^2$, $\mathrm{w}_6(\boldsymbol{q}_{\|}) = \left(\frac{\pi^5\hbar^4\Delta^2\wedge^2}{A_0 m^* L^6}\right)\exp(-\boldsymbol{q}_{\|}^2\wedge^2/4)$. Here n_s is a sheet impurity density, A_0 is the interface area; Δ and $\wedge$ are respectively the average height and correlation length of the interface roughness fluctuations.

In order to solve Eq. (1), $F_n(\boldsymbol{k}_{\|})$ can be presented as the sum of a symmetric $F_n^+(\epsilon_n)$ and an antisymmetric $F_n^-(\boldsymbol{k}_{\|})$ function, $F_n(\boldsymbol{k}_{\|}) = F_n^+(\epsilon_n) + F_n^-(\boldsymbol{k}_{\|})$ [4]. The action of the scattering operator on the antisymmetric part of the distribution function is described by the electron momentum relaxation time, which is usually introduced by means of the equation.

$$\hat{\mathrm{I}}F_n^-(\boldsymbol{k}_{\|}) = -\frac{F_n^-(\boldsymbol{k}_{\|})}{\tau_n^{(i)}(\epsilon_n)} \qquad (2)$$

(i). ***Acoustic phonon scattering:*** If the lattice temperature T is not very low, $k_0T > \sqrt{8m^*s_L^2W_0}$, then the electron-phonon interaction can be treated as quasielastic and in this case the momentum relaxation times in Eq. (2) will have the following forms: $\frac{1}{\tau_n^{(1)}(\epsilon_n)} = \frac{\pi\hbar}{m^*L\lambda_a}\left[Z(\epsilon_n) + \frac{1}{2}\right]$ for DA phonons, where $Z(\epsilon_n) = int[\sqrt{\epsilon_n/W_0}]$, and

$\frac{1}{\tau_n^{(2)}(\epsilon_n)} = \frac{1}{\tau_p}\frac{2k_0T_0}{\sqrt{2m^*s_T^2\epsilon_\parallel}}$ for PA phonons. Here $\lambda_a = \pi\hbar^4\rho s_L^2/m^{*2}E_a{}^2k_0T$ is a bulk electron mean free path due to DA phonon scattering, $\tau_p = 2\pi\rho\hbar^2 s_T/m^*e^2h_{14}^2$ is a characteristic scattering time for the bulk material due to PA phonon scattering and $\epsilon_\parallel = \hbar^2k_\parallel^2/2m^*$..

(ii). ***Polar optical phonon scattering:*** At room temperature the interaction with polar optical (PO) phonons via an absorption process becomes increasingly important in spite of the fact that the optical phonon occupation number PO phonon distribution function N_0 is still exponentially small, $N_0 = \exp(-\hbar\omega_0/k_0T)$. This is due to the very high polarity of the GaN material. In this case the momentum relaxation time which is almost independent of the electron energy is given as: $\frac{1}{\tau_n^{(3)}(\epsilon_n)} = 3\sqrt{\frac{W_0}{\hbar\omega_0}}N_0\frac{1}{\tau_0}$. Here $\tau_0 = e\hbar^2/(\epsilon_\infty^{-1} - \epsilon_0^{-1})e^2p_0$ and $p_0 = \sqrt{2m^*\hbar\omega_0}$.

(iii). ***Background and remote impurity scattering:*** In this case the only intrasubband terms are important because for intersubband terms $q_\parallel$ is large and the form-factor is exponentially small. Here the momentum relaxation times are similar to [5, 6]: $\frac{1}{\tau_n^{(4)}(\epsilon_n)} = \frac{\pi e^4N_IL}{\epsilon_0^2\hbar\epsilon_\parallel}\left[\pi - \frac{1}{2k_\parallel L}\ln(\sqrt{1+b_0} - b_0)\right]$ for background impurities, where $b_0 = \epsilon_0\epsilon_\parallel/e^2N_I^{1/3}$ and N_I is the bulk impurity density, and $\frac{1}{\tau_n^{(5)}} = \frac{\pi e^4N_s}{\epsilon_0^2\hbar\epsilon_\parallel}[I_0(4k_\parallel z_d) - L_0(4k_\parallel z_d)]$ for remote impurity scattering. Here N_s is a sheet impurity density $I_0(x)$ and $L_0(x)$ are modified Bessel and Struve functions, respectively and z_d is a position of remote ($|z_d| > L/2$) impurities. For background impurities z_d is integrated over space.

(iv). ***Interface roughness scattering:*** In this case the intersubband terms are equal to zero and the momentum relaxation time due to intrasubband scattering is calculated similar to [7] as $\frac{1}{\tau_n^{(6)}} = \frac{\pi^5\Delta^2\Lambda^2\hbar}{m^*L^6}\exp(-k_\parallel^2\Lambda^2/2)[I_0(k_\parallel^2\Lambda^2/2) - I_0(k_\parallel^2\Lambda^2/2)]$.

Using the momentum relaxation time approximation, the antisymmetric distribution is found in the form $F_n^-(\boldsymbol{k}_\parallel) = \frac{e\hbar}{m^*}\tau_n(\epsilon_n)(\boldsymbol{k}_\parallel.\boldsymbol{E})\frac{dF_n^+(\epsilon_n)}{d\epsilon_n}$ where the total momentum relaxation time $\tau_n(\epsilon_n)$ is defined as: $\tau_n(\epsilon_n) = (\lambda_a/\sqrt{2W_0/m^*})\chi_n(\epsilon_n)$ with $\chi_n(\epsilon_n) = [(z(\epsilon)+0.5) + (\lambda_a/\sqrt{2W_0/m^*})\sum_{i=2}^{6}(\tau_n^{(i)}(\epsilon_n))^{-1}]^{-1}$.

III. MOBILITY IN TERMS FOR GAN QUANTUM WELL AND BULK GAN

As shown in Fig. 1, the mobility due to intersubband transitions of electrons due to different types scattering (BI, DA, IR, PA, PO, RI) for QW can be obtained from the phenomenological relation:

$\mu = e\tau_n{}^{(i)}/m^*$ (3)

where m^* is the effective mass of GaN and $\tau_n{}^{(i)}$ is the momentum relaxation time of electrons. Using the same Eq. 3 the mobility due to different types of scattering (BI, DA, PA, PO) for bulk are obtained and shown in Fig. 2. The mobility in GaN QW and bulk GaN due to total scattering is also calculated and compared.

For calculation, following values of GaN parameters are used: m* = 0.15m$_0$, E$_a$ = 10.1eV, h$_{14}$ = 4.24 x 10^7 V/cm, ϵ_0 = 9.5, ϵ_∞ = 5.4, ρ = 6.1g/cm^3, S_L = 4.57 x 10^5 cm/s, $S_T \approx 0.5S_L$, $\hbar\omega_0$ = 92.8meV. To add some imperfections we have also used the parameters N_I = 10^{16} cm^{-3} for BI

scattering $Ns = 10^{11}$ cm^{-3} and Z_d = (L+500) Å for RI scattering and Λ = 20Å and Δ = 2Å for IR scattering.

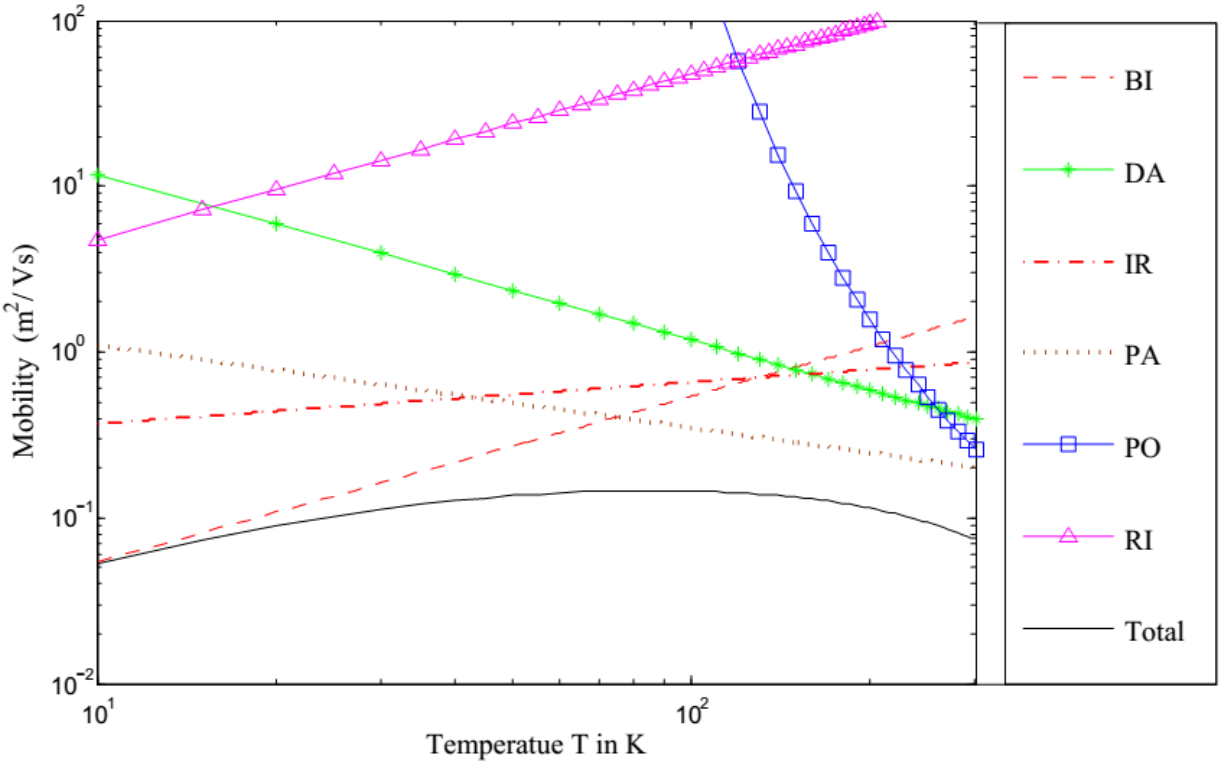

Fig. 1 Mobility of electrons versus temperature for a GaN QW of thickness (L) 50 Å

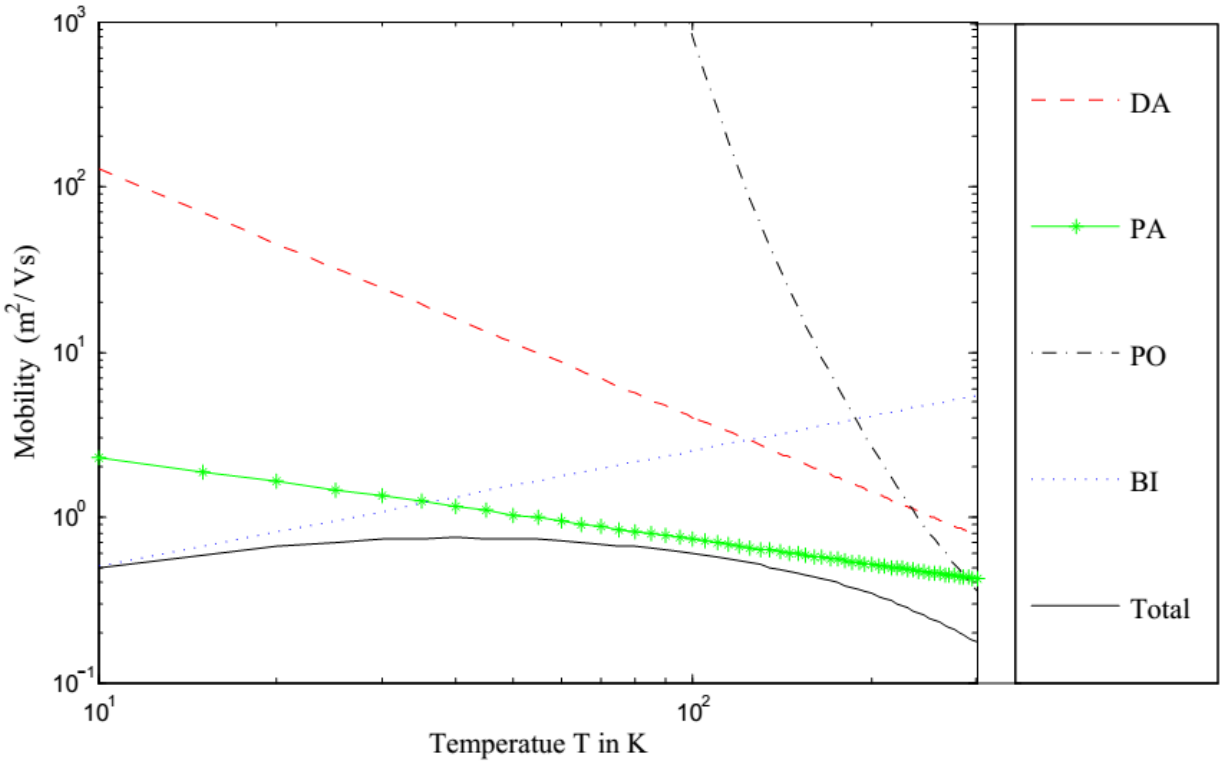

Fig. 2: Mobility of electron versus temperature for bulk GaN

It is clear from Fig. 1 and Fig. 2 that the mobility due total scattering in case of GaN QW is lesser than the value of bulk GaN. The main thing to note is that in case of bulk GaN, at higher temperature the mobility decreases faster than the case of GaN QW.
By stacking alternate layers of AlGaN and GaN of layer thickness d_1 and d_2 respectively, a periodicity is created along the growth direction with the periodicity length $D = d_1 + d_2$ for the binary alloy superlattice AlGaN/GaN.
Now, by using following relation conductivity can be calculated

$$\sigma = Ne\,\mu \qquad (4)$$

where N is the electron concentration and is taken as 10^{12} m^{-2}. The conductivity is calculated for both bulk and superlattice phonons for various lattice temperature and the results have been displayed in the Fig. 3.

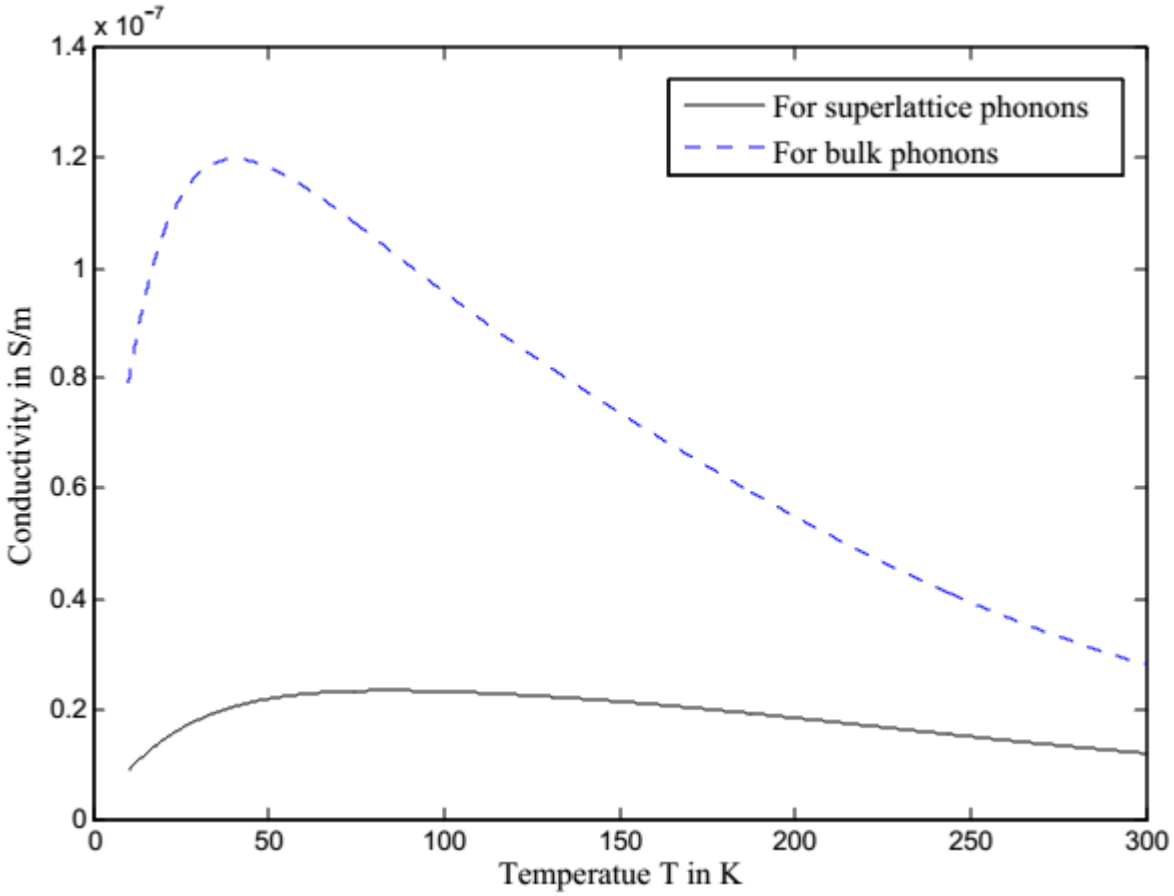

Fig. 3: Variation of conductivity with lattice temperature T in AlGaN/GaN MOSFET

From Fig. 3, it is clear that at low temperature the difference between the conductivity of superlattice and bulk material is large and at high value of temperature the difference is small. At the 40 K of the lattice temperature the difference between the conductivity of superlattice and bulk material is 9.958 x 10^{-8} S/m, which is the highest difference.
Next the calculations of power dissipation are made and have studied its variation with increasing lattice temperature T for both bulk and superlattice phonons. The relation for power dissipation in the superlattice is given as:

$$P = \sigma E^2 \qquad (5)$$

where E is the electric field given by

$$E = V/d_2 \qquad (6)$$

V is the potential and for our calculations *V* = 0.1 mV. The plots for power dissipation are shown in Fig. 4. And it is to be noted that the highest difference between the power dissipation of superlattice and bulk is 9.958 W which is at 40 K value of temperature. At lesser value of 40 K the power dissipation increases monotonically for both bulk and superlattice phonons. But after 40 K the power dissipation in bulk is almost constant where as in case superlattice the power dissipation decreases rapidly.

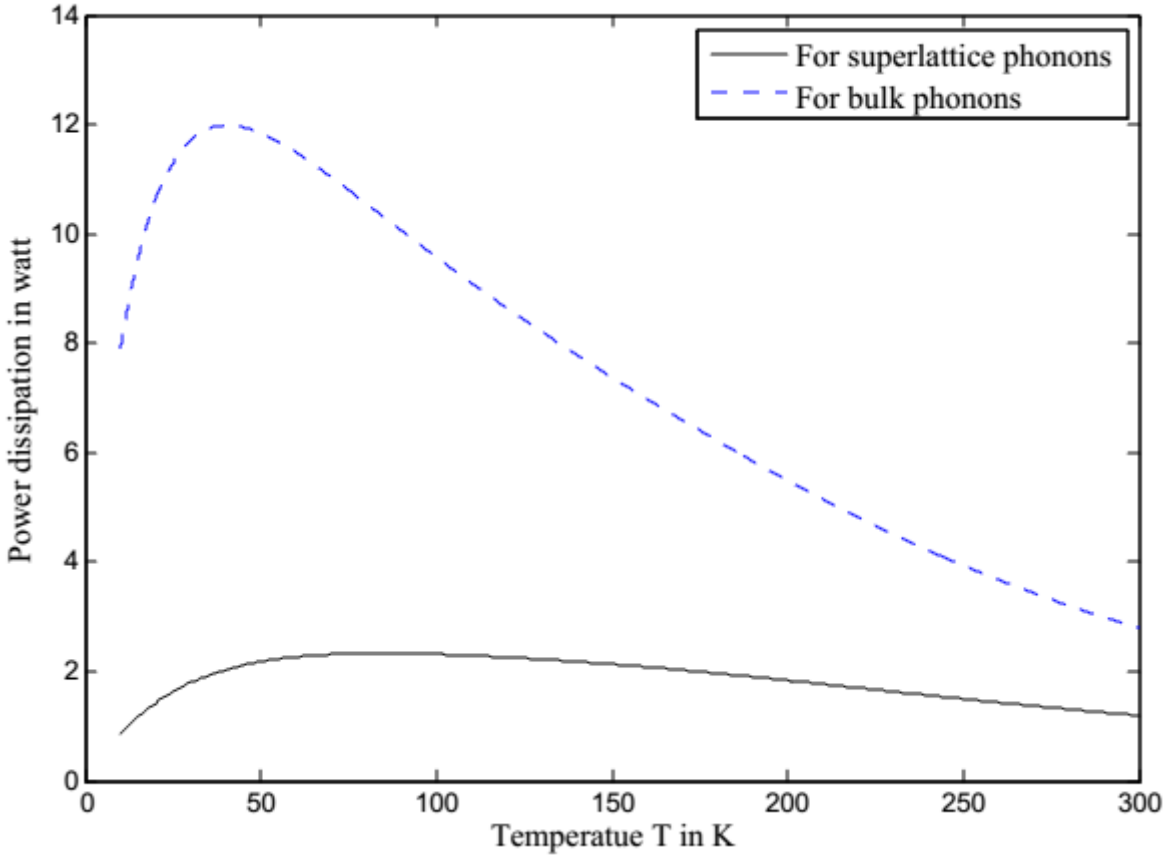

Fig. 4: Variation of power dissipation with temperature in MOSFET

IV. MODEL OF SUPERLATTICE MOSFET

An array of GaN quantum-wells with layers of AlGaN barriers has been fabricated over a Si substrate to form a MOSFET. As shown in the Fig. 5 there are 10 alternate layers of AlGaN/GaN. The thickness of GaN is 10 nm and of AlGaN is 20nm, which have been implanted on Si substrate. Thus a total thickness of 250 nm of AlGaN/GaN superlattice structure for the MOSFET has been designed.

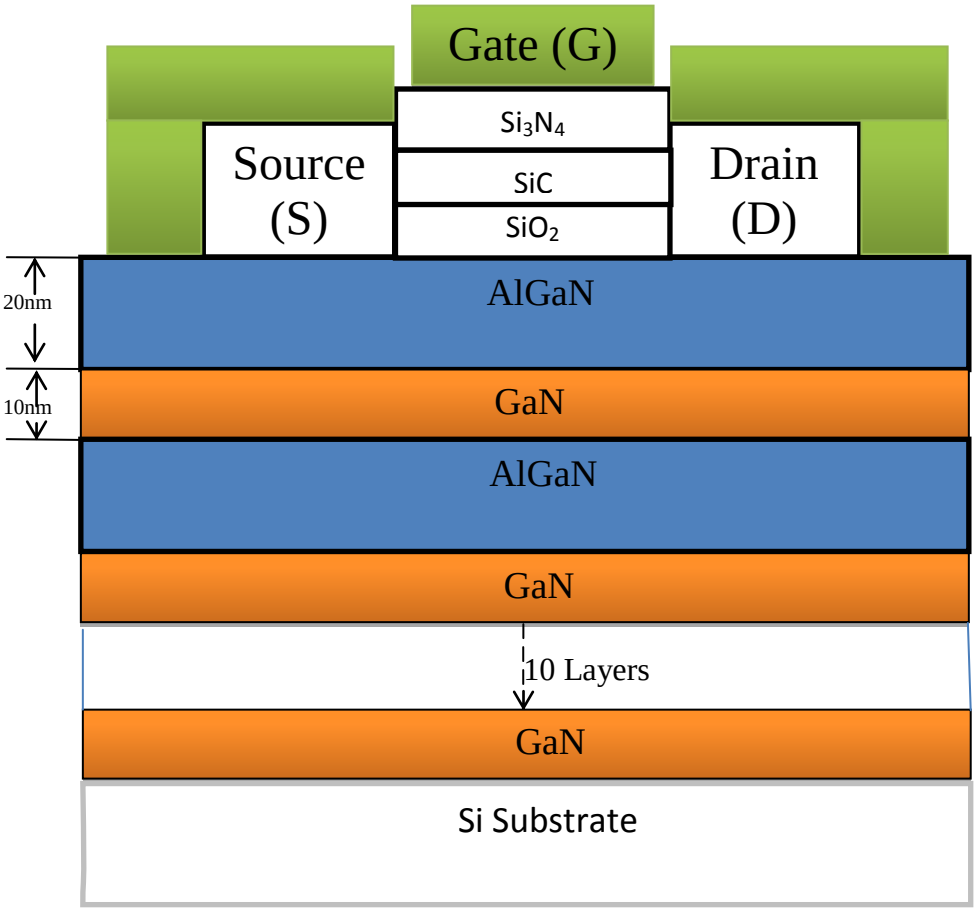

Fig. 5: Structure of superlattice MOSFET

On application of drain voltage (V) the drain current (J) is controlled by the relation:

$J = Ne\mu E$ *(7)*

where E= V/d_2 is the applied electric field. We rewrite the equation (7) in the terms of conductivity (σ) as follows:

$J = \sigma E$ *(8)*

The variation of drain current (at constant drain voltage) with respect to temperature for both bulk and superlattice due to total phonons scattering is characterized in Fig. 6.

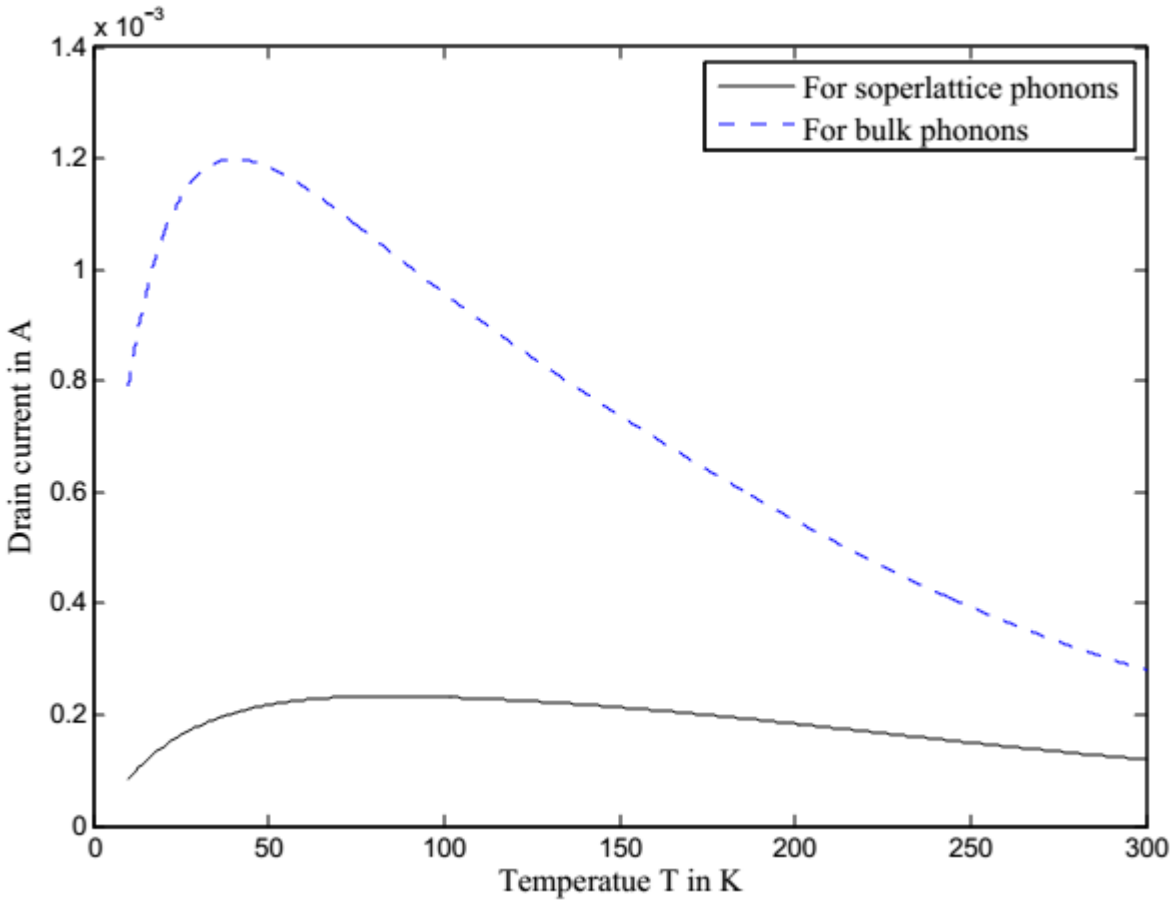

Fig. 6: Drain current versus lattice temperature characteristics for both superlattice and bulk phonons

It is clear from Fig. 6 that in case of GaN superlattice the drain current increases monotonically up to 40 K of the lattice temperature and after 40 K it decreases rapidly whereas in case of bulk GaN initially it increases slowly and in between 50 K and 100 K drain current is almost constant and after 100 K it decreases slowly.

V. CONCLUSION

In the present communication the authors have shown the variations of mobility with lattice temperature due to different scattering mechanisms for both GaN QW and bulk. The conductivity of bulk and superlattice phonons mediated by intersubband transitions of electrons with the lattice temperature for GaN/AlGaN superlattice has been studied. The conductivity is found to be high at low value of lattice temperature. The variations of power dissipation with lattice temperature has been studied which reveals that for superlattice phonons the power dissipation is comparatively smaller than that of bulk. Also a AlGaN/GaN superlattice MOSFET is designed theoretically and corresponding drain current versus lattice temperature characteristics has been studied.

References

1. K. Mazumdar, A. Biswas and A. Ghosal, "Study of conductivity and power dissipation in GaAlAs/GaAs superlattice due to electron-phonon interaction", Journal of Elect. Devices, **15**, 1232 (2012).
2. Kaushik Mazumdar, Abhishek Jha, Reshma Begum, Aniruddha Ghosal, "Mobility of 1-D GaAs Quantum Wire Limited by Polar Optic Phonon Scattering", International Journal of Innovative Research in Sci. Eng. and Tech. **3**, 638 (2014).
3. Kaushik Mazumdar, Vishwanath Pratap Singh, Aniruddha Ghosal, "Noise Analysis In Short Channel AlGaN/AlN/GaN HEMT", International Journal of Innovative Research in Sci. Eng. and Tech. **5**, 9 (2014).
4. N. A. Zakhleniuk, C.R. Bennett, B.K.Ridley, and M. Babiker, "Multisubband hot-electron transport in GaN-based quantum wells", Appl. Phys. Lett. **73,** 2485 (1998).
5. B. K. Ridley, Quantum Processes in Semiconductors (Clarendon Press, Oxford, 2nd ed. 1988).
6. J. Lee, H. N. Spector and V. K. Arora, "Impurity scattering limited mobility in a quantum well heterojunction", J. Appl. Phys. **54,** 6995 (1983).
7. H. Sakaki, T. Noda, K. Hirakawa, M. Tanaka and T. Matsussue, "Interface Roughness Scattering in GaAs/AlAs Quantum Wells", Appl. Phys. Lett. **51,** 1934 (1987).